

Electronic Supporting information

Synthesis, characterization and cytotoxicity of europium incorporated ZnO-graphene nanocomposites on human MCF7 breast cancer cells

Susanta Bera¹, Monisankar Ghosh^{2#}, Moumita Pal^{1#}, Nilanjana Das¹, Suchandrima Saha², Samir Kumar Dutta² and Sunirmal Jana^{*1} (#Authors contributed equally to this work)

¹Sol-Gel Division, CSIR-Central Glass and Ceramic Research Institute, 196 Raja S.C. Mullick Road, P.O. Jadavpur University, West Bengal, Kolkata 700032, India.

²Drug Development Diagnostic & Biotechnology, CSIR-Indian Institute of Chemical Biology, 4 Raja SC Mullick Road, P.O. Jadavpur University, West Bengal, Kolkata 700032, India.

Synthesis of graphene oxide (GO)

Following modified Hummer's method¹, graphene oxide (GO) was prepared from graphite powder (<20 micron, Sigma Aldrich). In a brief synthesis, ~5 g graphite powder, 2.5 g NaNO₃ (Merck, 99%) and 150 mL concentrated H₂SO₄ (Merck, 98%, GR) were mixed together by stirring and placed the container in an ice bath for 3 h. Then, 20 g of KMnO₄ (Merck, 98.5%) was added slowly and kept the aliquot under stirring condition for further 1 h. After that the mixture was stirred vigorously followed by addition of 250 mL distilled water. Then, the reaction mixture was kept for 30 min at 98±2°C. After that it was mixed with 500 mL of warmed distilled water followed by slow addition of 10 mL of H₂O₂ (30 wt%, Merck). Finally, the product was separated by centrifugation using 250 mL aqueous HCl solution (10:1, v/v) and subsequently washed with distilled water (5 times). After drying at 55°C, the solid mass appeared as blackish brown non-shiny material.

1. W. S. Hummers, R. E. Offeman, *J. Am. Chem. Soc.*, 1958, **80**, 1339.

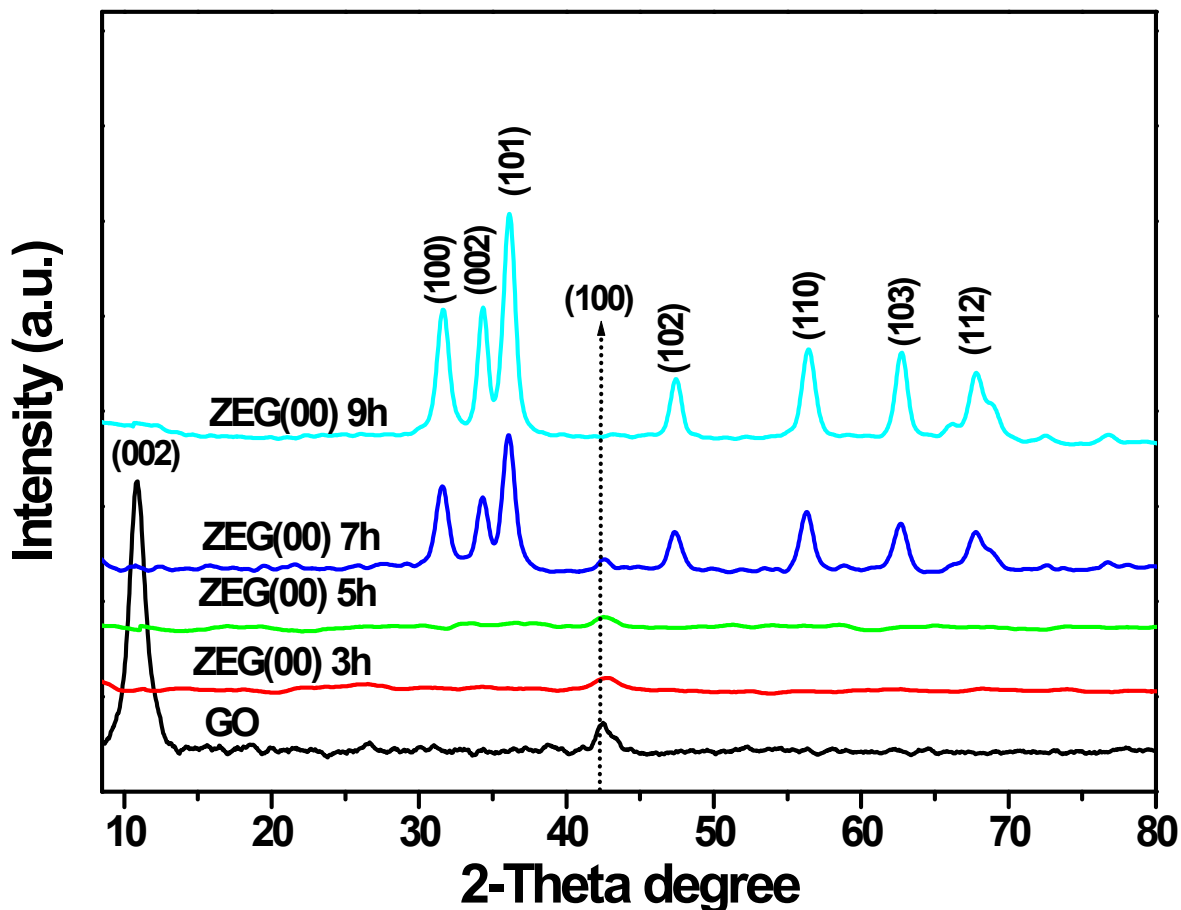


Fig. S1: XRD patterns of ZEG(00) nanocomposites synthesized at different reaction times. With increasing reaction time, the intensity of the characteristics XRD 2θ peaks of GO, located at 10.9° and 42.4° gradually decreased. After 7 h reaction time, the formation of hexagonal ZnO was evidenced. Finally, after 9 h of reaction progress, the XRD peaks for GO found to disappear with the further increase of intensity of diffraction peaks for hexagonal ZnO. This could demonstrate the complete conversion of GO to chemically converted graphene (CCG) took place in the nanocomposite after 9 h reaction time.

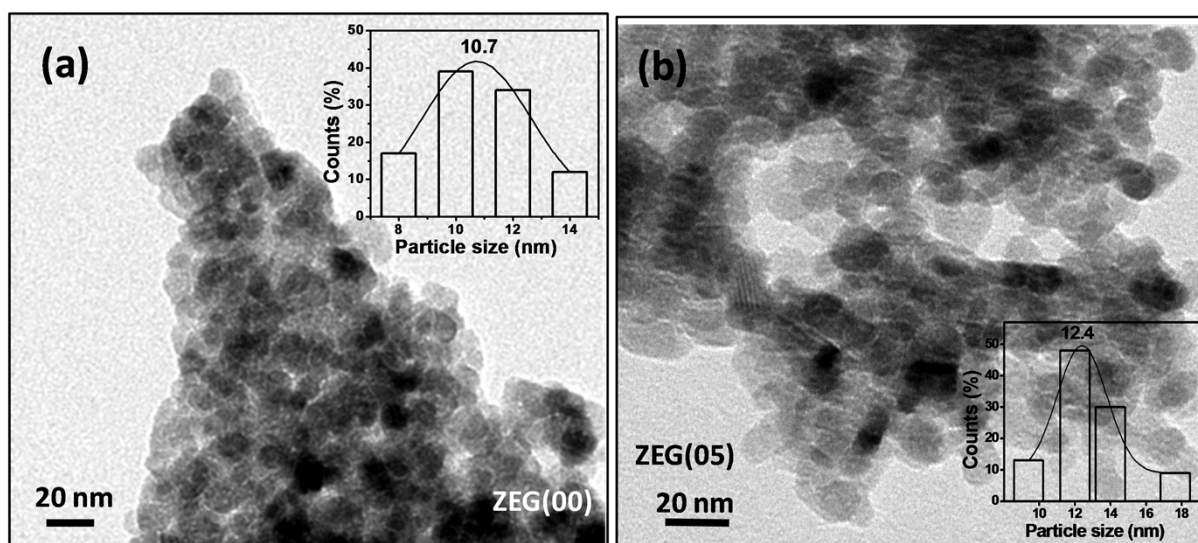


Fig. S2: TEM images and histograms (insets) showing the particle size distributions of (a) ZEG(00) and (b) ZEG(05), respectively.

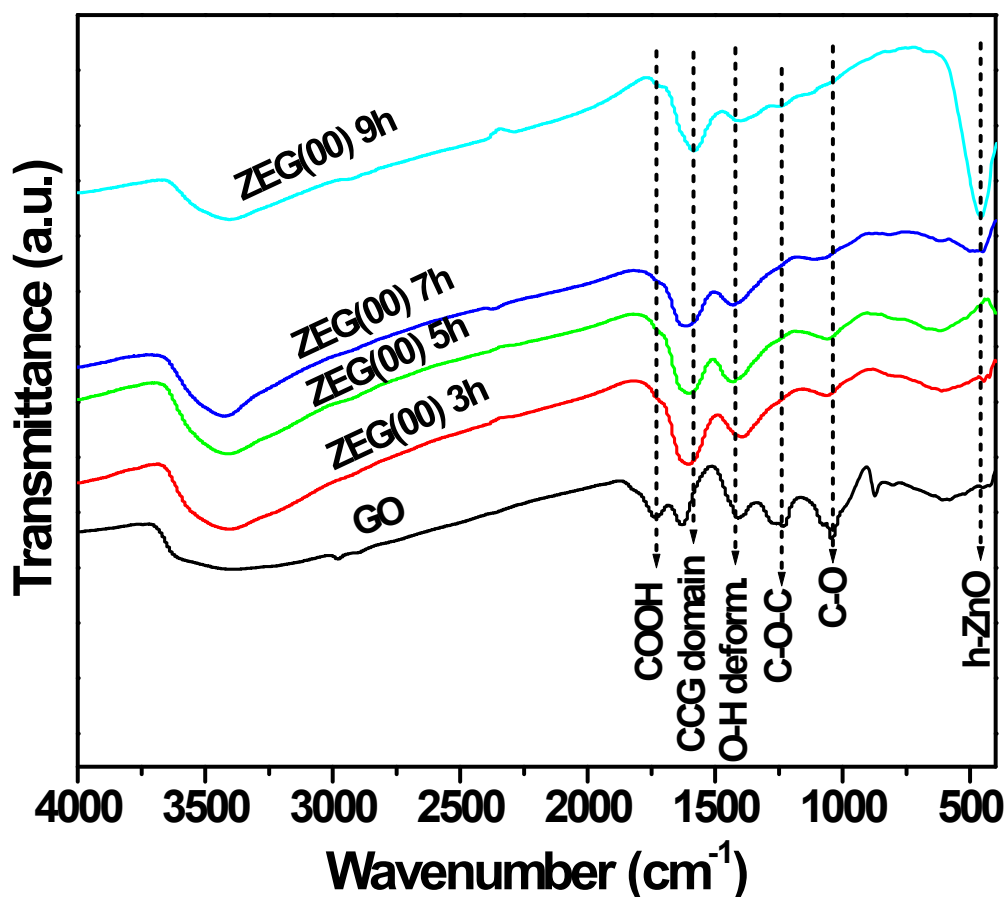


Fig. S3: FTIR spectra of ZEG(00) nanocomposite synthesized at different reaction times. As seen from the figure, on increasing reaction time, the intensity of FTIR vibrations related to oxygen functionalities of GO decreases to a large extent. However, at 9h reaction time, two additional peaks appeared at $\sim 1570 \text{ cm}^{-1}$ and $\sim 460 \text{ cm}^{-1}$ which could correspond^{1,2} to graphitic domains of chemically converted graphene and hexagonal ZnO, respectively. The other vibrations related to GO and CCG are shown in the figure.

1. Q. Zhang, C. Tian, A. Wu, T. Tan, L. Sun, L. Wang, H. Fu, *J. Mater. Chem.*, 2012, **22**, 11778–11784.
2. S. Bera, M. Pal, S. Sarkar, S. Jana, *Appl. Surf. Sci.*, 2013, **273**, 39–48.

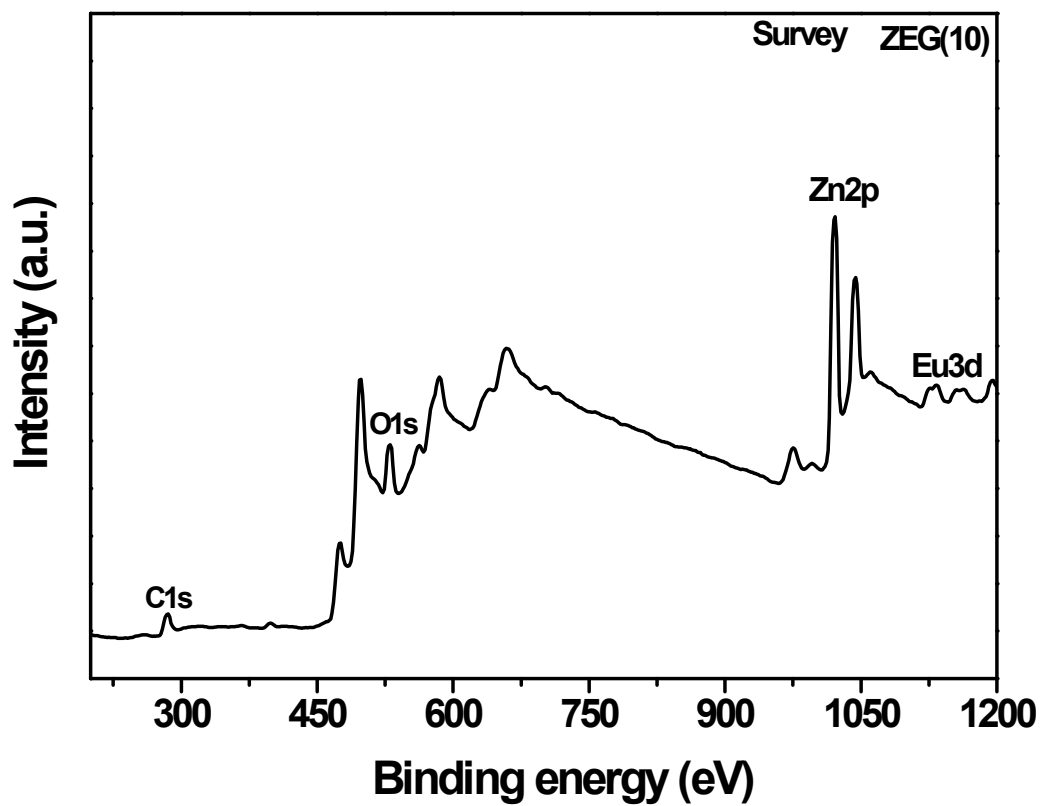


Fig. S4: XPS survey spectrum (binding energy range, 200-1200 eV) of ZEG(10). The presence of carbon, oxygen, Zn^{2+} and $\text{Eu}^{3+}/\text{Eu}^{2+}$ was detected from their respective binding energy signals.

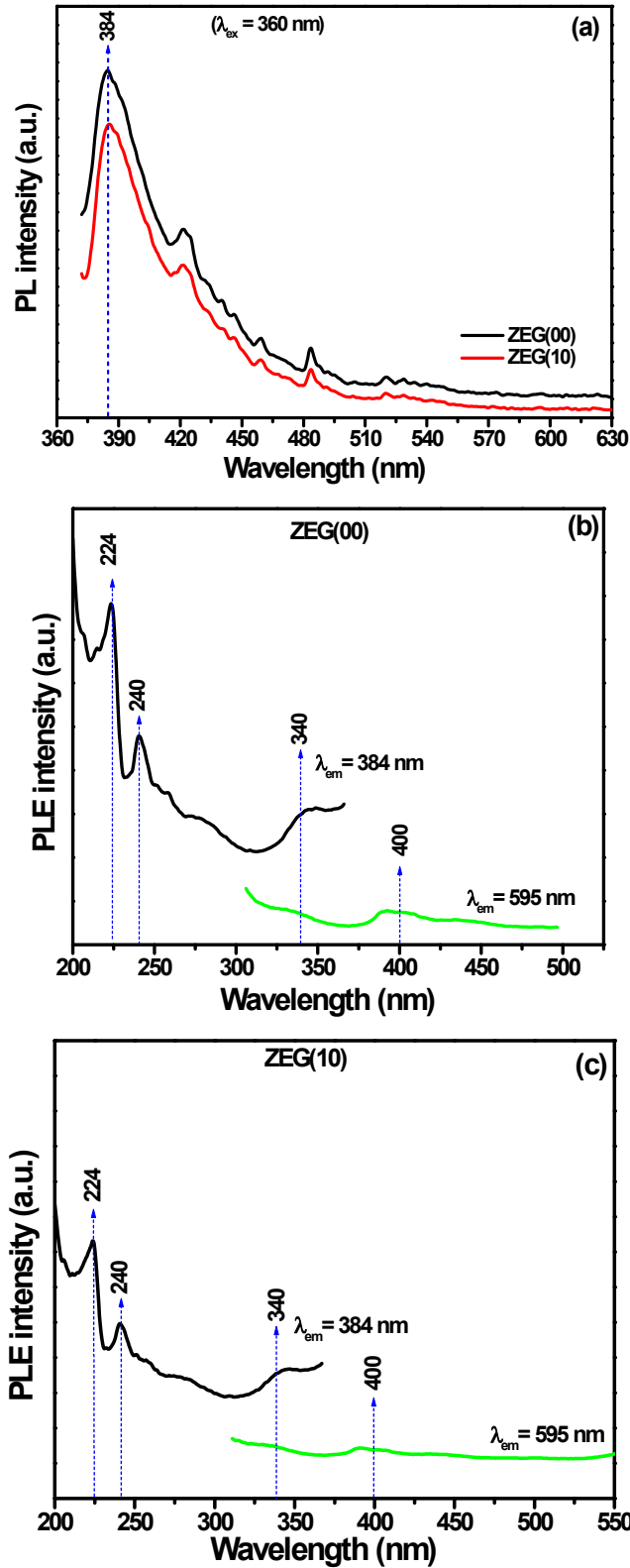


Fig. S5: (a) Photoluminescence (PL) emission spectra ($\lambda_{ex} = 360$ nm) of ZEG(00) and ZEG(10) nanocomposites. (b) and (c) represent the photoluminescence excitation (PLE) spectra fixing emission at 384 nm and 595 nm of (b) ZEG(00) and (c) ZEG(10) samples, respectively.

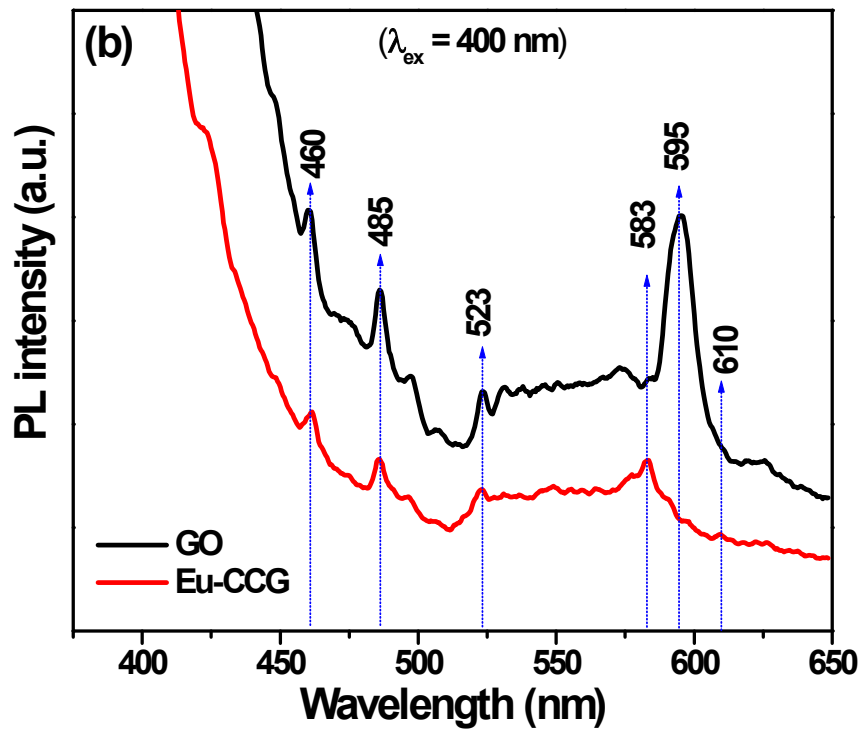
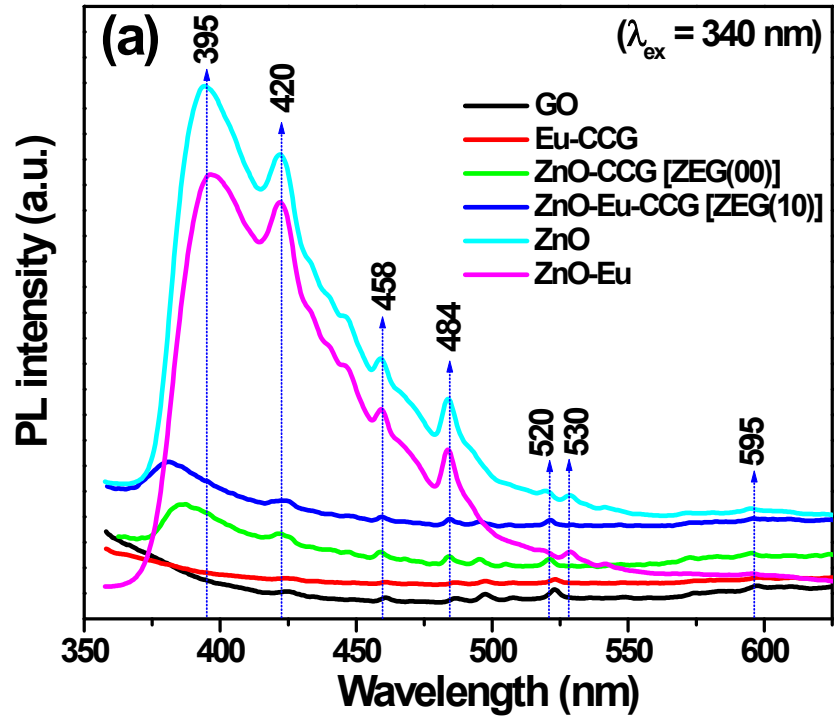


Fig. S6 (a), (b)

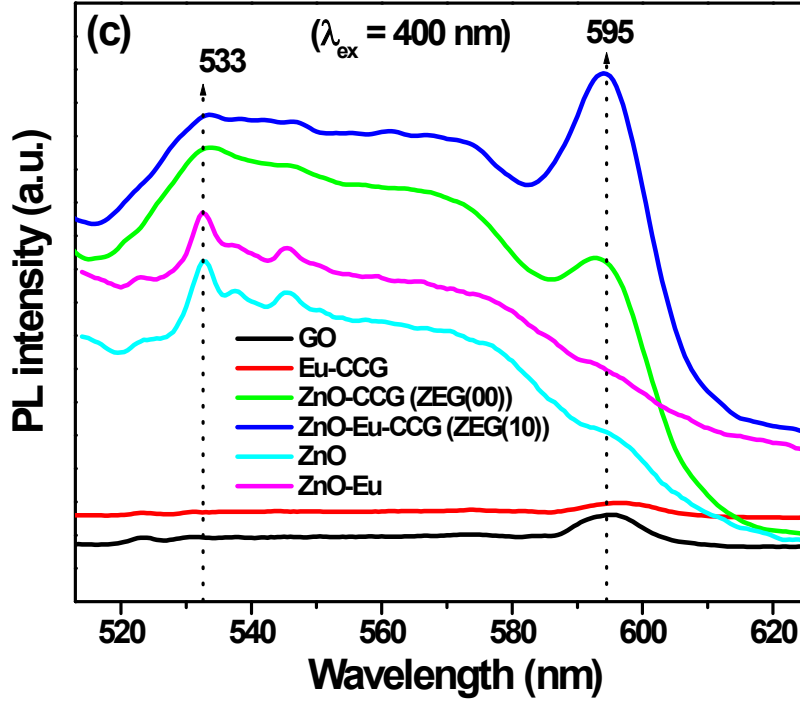


Fig. S6: Photoluminescence (PL) emission spectra of pure and composite materials at different excitation wavelengths, (a), $\lambda_{\text{ex}} = 340$ nm; (b) and (c), $\lambda_{\text{ex}} = 400$ nm.

It could be noted that graphene oxide (GO) due to its numerous disorder-induced defects exhibits prominent visible emissions¹. In the present work, except the PL peak at ~ 385 nm, a series of visible emissions ($\lambda_{\text{ex}} = 340$ nm and 400 nm) including the PL peak at ~ 595 nm in GO were also observed. It should be mentioned that all the PL spectra were recorded at fixed measurement condition. However, a very low intensity of the PL peaks in GO were found compare to the ZnO based nanocomposites. The GO was found to be converted to CCG in ZEG samples including ZnO-CCG (ZEG(00)) as evidenced from XRD, FTIR and Raman measurements. Also, the PL spectrum (**Fig. S6b**) of Eu-CCG confirmed the conversion of GO to CCG where the PL peak at 595 nm (orange emission) was nearly disappeared but a new peak at 583 nm was appeared, attributed to $^5D_0 - ^7F_0$ transition of europium². In addition, a weak peak appeared at ~ 610 nm, ascribed to $^5D_0 - ^7F_2$ transition.² However, in ZnO-CCG (ZEG(00)), the intensity of the orange emission (assigned to interstitial oxygen)³

was noticed to be stronger than the pure ZnO or ZnO-Eu composite. These results suggested that apparently, there might not be a contribution coming from ZnO in the enhancement of the intensity (defect density) of the orange emission. However, it was already evident that the orange emission was nearly disappeared when GO converted to CCG in Eu-CCG^{1,4}. Moreover, the XRD and other studies also favoured the conversion of GO to CCG in ZEG(00) nanocomposite. Thus, it could conclude that CCG would assist in combination with Eu to enhance the orange emission in ZnO and the maximum enhancement of the emission intensity was found in ZEG(10). As XPS (**Fig. 5**) study already confirmed the formation of Eu²⁺ ions in the nanocomposite, perhaps the Eu²⁺ ions in an optimum concentration might be playing a significant role² for the enhancement of the PL intensity at 595 nm.

1. C.-T. Chien, S.-S. Li, W.-J. Lai, Y.-C. Yeh, H.-A. Chen, I-S. Chen, L.-C. Chen, K.-H. Chen, T. Nemoto, S. Isoda, M. Chen, T. Fujita, G. Eda, H. Yamaguchi, M. Chhowalla and C.-W. Chen, *Angew. Chem. Int. Ed.*, 2012, **51**, 6662–6666.
2. X. Zeng, J. Yuan and Z. Wang, L. Zhang, *Adv. Mater.*, 2007, **19**, 4510–4514.
3. L. E. Greene, M. Law, J. Goldberger, F. Kim, J. C. Johnson, Y. Zhang, R. J. Saykally and P. Yang, *Angew. Chem. Int. Ed.*, 2003, **42**, 3031–3034.
4. B. K. Gupta, P. Thanikaivelan, T. N. Narayanan, L. Song, W. Gao, T. Hayashi, A. L. M. Reddy, A. Saha, V. Shanker, M. Endo, A. A. Marti, P. M. Ajayan, *Nano Lett.*, 2011, **11**, 5227-5233.

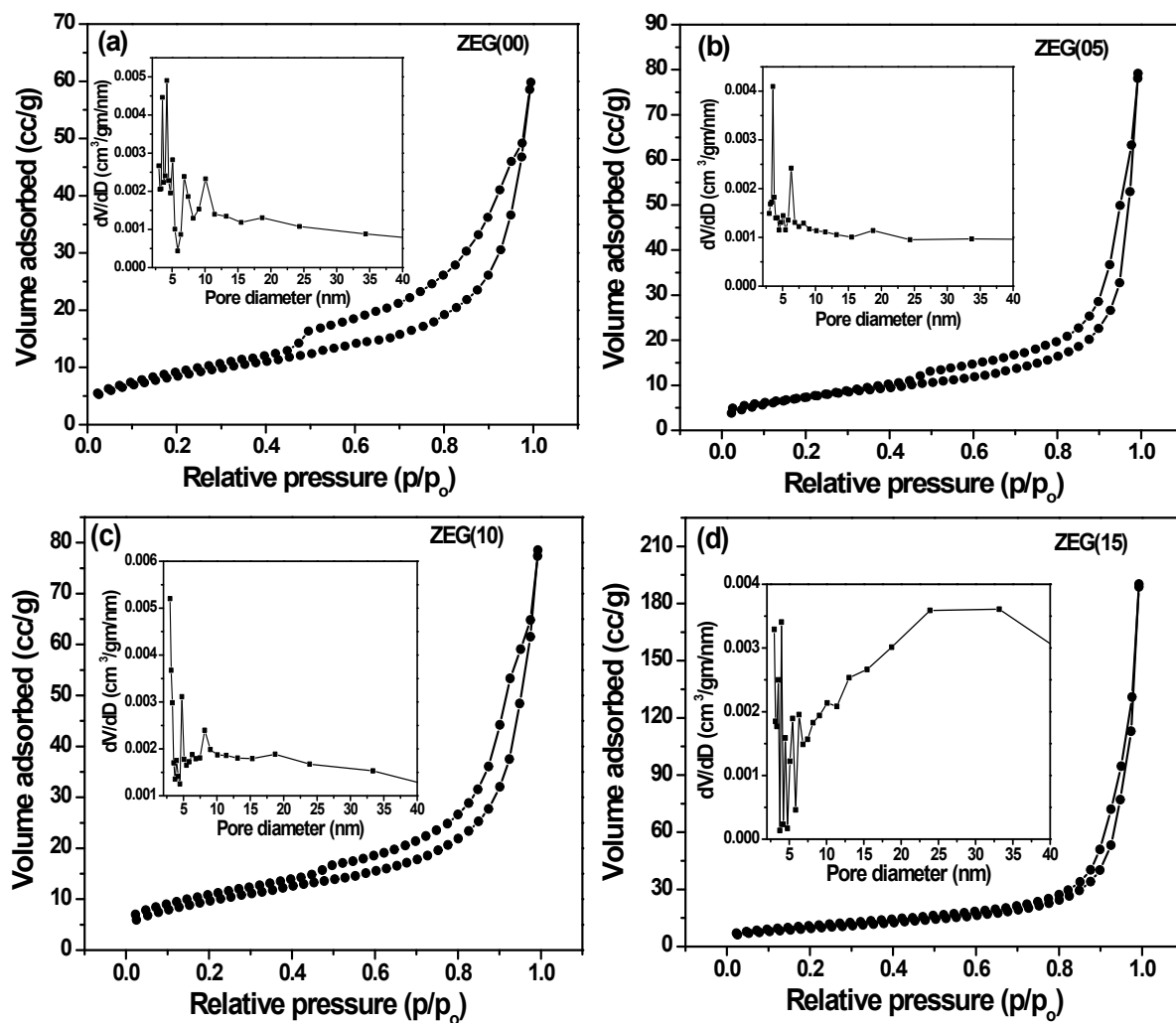


Fig. S7: BET nitrogen adsorption and desorption isotherms of ZEG nanocomposites. Insets show the respective multi-modal pore size distribution curve.

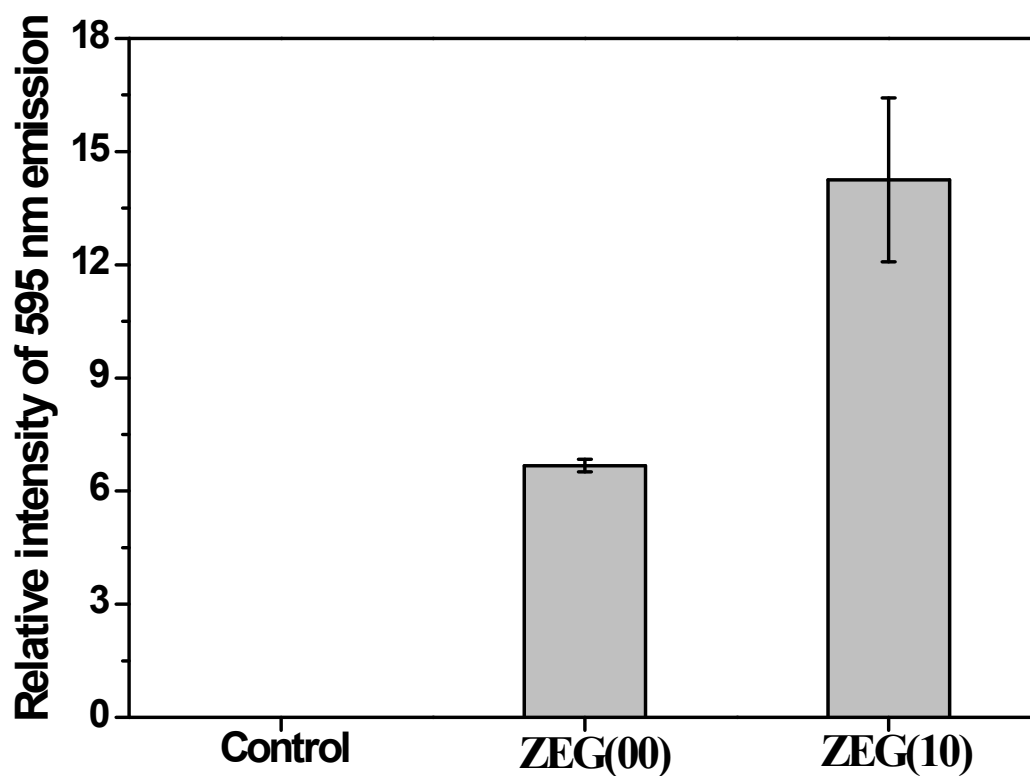


Fig. S8: Relative brightness of cell images from orange light emission using ZEG(00) and ZEG(10) nanocomposites. Intensity of the respective cell images were calculated by ImageJ software.

Table S1: I_D/I_G values (including precursor graphene oxide, GO) calculated from Raman spectra of nanocomposites

| Sample ID | FWHM (cm⁻¹) | I_D/I_G |
|------------------|-------------------------------|-----------------------------|
| GO | 97 | 0.79 |
| ZEG(00) | 102 | 0.92 |
| ZEG(05) | 114 | 0.98 |
| ZEG(10) | 122 | 1.00 |
| ZEG(15) | 120 | 1.00 |

Table S2: Pore size, pore volume and surface area of ZEG nanocomposites measured from BET nitrogen isotherm

| Sample designation | Average pore diameter (nm) | Specific surface area (m²/g) | Average pore volume (cc/g) |
|---------------------------|-----------------------------------|--|-----------------------------------|
| ZEG(00) | 11.9 | 31.1 | 0.0925 |
| ZEG(05) | 18.5 | 26.4 | 0.1225 |
| ZEG(10) | 13.6 | 35.6 | 0.1215 |
| ZEG(15) | 34.1 | 34.5 | 0.2942 |